

SEL EXHIBIT NO. 2038

INNOLUX CORP. v. PATENT OF SEMICONDUCTOR ENERGY
LABORATORY CO., LTD.

IPR2013-00066

18:3: Late-News Paper: Polarization Independent Liquid Crystal Microdisplays

Ravi K. Komanduri, Chulwoo Oh, and Michael J. Escuti

Dept of Electrical & Computer Engineering, North Carolina State University, Raleigh, NC 27695

D. Jason Kekas

ImagineOptix Corporation, 7202 Doverton Court, Raleigh, NC 27615

Abstract

We demonstrate a polarization-independent, diffractive, liquid crystal microdisplay on a reflective 256x256 pixel silicon backplane using nematic liquid crystal polarization gratings. Striking results are observed in a single-panel projector with remarkably simple optics, where the technology supports up to ~75% throughput (reflectance) of unpolarized light, contrast ratios approaching 1000:1, and < 800 μ s total switching time.

1. Introduction

Our objective is to develop a viable liquid crystal (LC) microdisplay inherently capable of modulating unpolarized light with strong contrast, for the purposes of highly efficient projection displays. Primary application contexts include ultra-portable and front-projection systems, and we aim to implement a field-sequential-color approach that would be particularly well suited to work with étendue-limited light engines (including but not limited to light-emitting-diodes). Here we specifically report on our success in building a 256x256 prototype LC microdisplay with a reflective silicon backplane based on switchable polarization gratings [1-4], which are capable of up to ~75% true throughput of unpolarized light, contrast ratios approaching 1000:1, and < 800 μ s total switching time.

Modulation of unpolarized light overcomes the unfortunate dependency of almost all LC displays on polarizers for high contrast. Most polarizer-free approaches suffer from poor contrast ratio and fabrication difficulties [5]. A family of binary LC gratings [6-8] and a class of holographically-formed polarization gratings (PGs) [9-11] were previously studied for this purpose but were plagued by severe scattering, were limited to small diffraction angles, and did not achieve high diffraction efficiencies (limiting contrast and brightness).

We first demonstrated experimentally transmissive liquid crystal polarization gratings (LCPGs) at SID 2006 with nearly ~100% diffraction efficiency and low scattering [1, 3]. We have since extended this approach to reflective substrates, and achieved good holograms on both aluminum (Al) mirrors and pixilated silicon (Si) backplanes. The advantages of the reflective mode (over transmissive mode) are many: half the required LC layer thickness enables faster switching speed [4], smaller grating periods, and larger diffraction angles.

Because of the above-mentioned advantages, we implemented a projection system using a single LCPG microdisplay and field-sequential-color, as illustrated in Fig. 1c. In this configuration, diffracting pixels (w/o voltage) send light around the fold-mirror to the screen, while non-diffracting pixels (w/ high voltage)

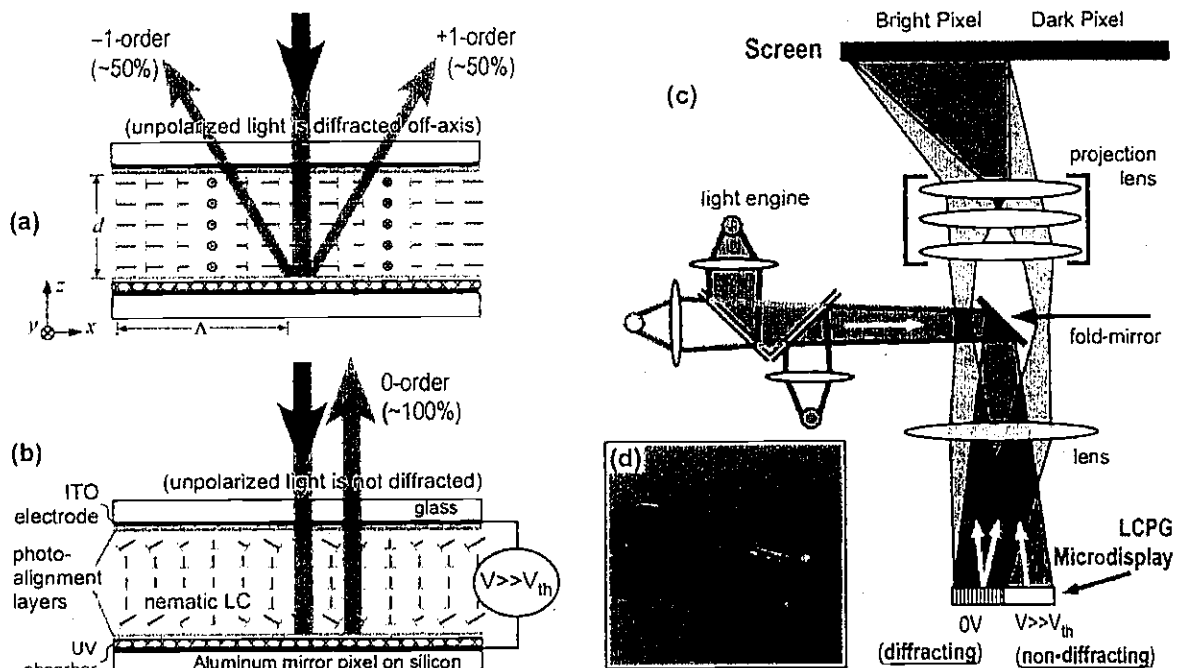
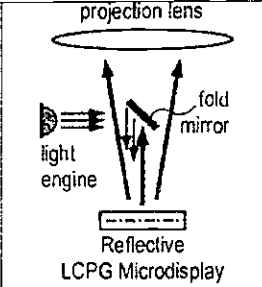
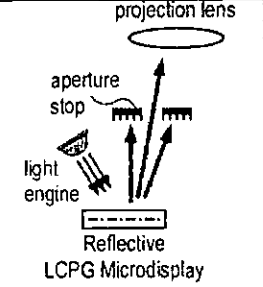
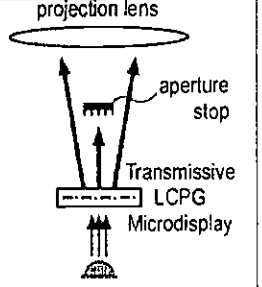
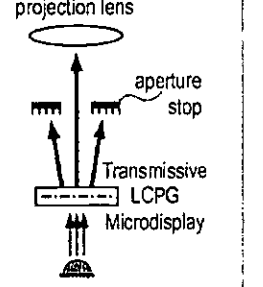


Figure 1 – The polarization-independent LCPG microdisplay: (a) Sub-pixel configuration (0V) of the nematic LC established by the photo-alignment layers, where only first-order diffraction occurs; (b) High voltage configuration, where out-of-plane alignment effectively erases the grating and light is reflected specularly; (c) Telcentric reflective projector system; (d) Photo of microdisplay.

Table 1 – A high-level comparison of efficient projector designs for LCPG microdisplays (assumptions described in text).

Category	Reflective		Transmissive	
	Mode	Configuration	Mode	Configuration
Design				
Mode	Reflective		Transmissive	
Configuration	Telecentric, Dark-Field	Non-Telecentric, Bright-Field	Telecentric, Dark-Field	Telecentric, Bright-Field
Raw Contrast Ratio	High ($\geq 1000:1$)	Low ($\sim 100:1$)	High ($\geq 1000:1$)	Modest ($\sim 200:1$)
Projection Lens F/#	Low (≤ 1)	Standard (~ 2)	Low (≤ 1)	Standard (~ 2)
Pixel Voltage Range	Modest ($\geq 15V$)	Low ($\leq 10V$)	High ($> 30V$)	Low ($\leq 10V$)
Pixel Fill-Factor	High ($\sim 93\%$)		Modest ($\sim 60\%$)	
Switching Time	Faster ($\sim 600 \mu s$)		Fast ($< 1 ms$)	
Optimum Application	Front-Projectors		Compact and Embedded Projectors	

reflect light directly back into the light source or toward an aperture stop.

It is important to note that LCPG microdisplay technology (in general) presents multiple configuration choices at the projector level, including: reflective or transmissive, telecentric or non-telecentric, and bright-field or dark-field [2]. In Table 1, we illustrate and compare the configuration studied here (see also Fig. 1(c)), along with three additional options in a best-case scenario (with first-order diffraction angle of $\pm 24^\circ$ and our currently-known materials). Reaching for an order-of-magnitude comparison, we estimate the trends of several key parameters, and assume that the illumination is unpolarized (from LEDs), operated with field-sequential-color, and has a $\pm 12^\circ$ divergence angle at the microdisplay (roughly 0.5° diagonal).

If the priority is high contrast and a larger projection lens is acceptable, as in front-projectors, then the reflective/telecentric/dark-field option is likely best. If the priority is a small package size and contrast requirements are relaxed, as in ultra-portable embedded projectors, then the transmissive/telecentric/bright-field option is likely best. While we employ reflective LCPGs in this work, many of the basic results would arise similarly in the transmissive-mode.

2. Reflective LCPG Properties

LCPGs comprise an in-plane, uniaxial birefringence [9, 11] that varies with position (i.e. $n(x) = [\sin(\pi x/\Lambda), \cos(\pi x/\Lambda), 0]$, as shown in Fig. 1). The most compelling features include $\sim 100\%$ diffraction into the first-orders regardless of polarization, and the presence of only the zero- and first-orders (the conventional grating equation applies). Using the Extended Jones Matrix method [12], we derive the ideal first-order diffraction efficiency in the reflective-mode illuminated by unpolarized light as

$$\eta_{\pm 1} = \eta_{\pm 1} = \frac{C}{2} \sin^2 \left(\frac{2\pi \Delta n d}{\lambda} \cos \theta \right) \quad (1)$$

$$C = (1/16) \cos^2 \theta (4 + 3 \sin^2 \theta) (8 - \cos^2 \theta (4 + 3 \sin^2 \theta)) \quad (2)$$

For small angles of incidence ($\leq 20^\circ$), $C \sim 1$ and $\eta_{\pm 1} \sim 50\%$, akin to transmissive operation [1]. Note, λ is the vacuum wavelength, Δn is the birefringence, d is the grating thickness (Fig. 1), and θ

is the incident angle of light within the LC. Nearly all incident light is diffracted into the first-orders at the quarterwave condition $d = \lambda/(4\Delta n)$, regardless of incident polarization. Note that an applied voltage above the threshold V_{th} (typ. ~ 2 V) reduces Δn , redirecting incident light into the zero-order. Both the first- and zero-orders can therefore be modulated between $\sim 0\%$ to $\sim 100\%$ for unpolarized light over a range of incident angles and λ .

3. Reflective LCPG Fabrication

Prior work on LCPGs has been solely focused (to our knowledge) on transmissive substrates [1, 9, 10]. Here we report our success in producing excellent quality LCPGs on Al mirrors and good quality gratings on reflective Si backplanes. Reflective fabrication is far more difficult than on transmissive substrates because the reflection of the holographic recording beams corrupts the interference throughout the recording volume (e.g. the intensity within the polarization hologram no longer remains constant). Therefore, our approach involves removing the reflection of the ultraviolet (UV) recording beams from the substrate using a UV absorbing layer, while otherwise following standard fabrication procedure [1, 9].

Fabrication involves the following basic steps: (1) The reflective substrate and ITO-glass (Delta Technologies) are cleaned with methanol; (2) The reflective substrate is spin-coated with a UV absorbing material (i.e. 9:1 wt/wt mix of Wide-15B (Brewer Science) and 2,2'-dihydroxybenzophenone (Sigma-Aldrich)) at 6000 rpm for 60 s, followed by a post-bake on a hotplate at $110^\circ C$; (3) Both substrates are coated with a photo-alignment material [13] ROP-103-2CP (Rolie), at 3000 rpm for 45 s, followed by the standard post-bake; (4) Substrates are joined together, where the cell gap is maintained with $1.1 \mu m$ silica spacers (Dana Enterprises) dispersed within the glue seal (Norland); (5) The assembly is then exposed to a UV polarization hologram from a HeCd laser (325 nm), with orthogonal circularly polarized beams (dose $\sim 0.5 J/cm^2$) at grating period $\Lambda \sim 2.6 \mu m$ (i.e. 14° diffraction angle at $\lambda = 632$ nm); (6) Finally, the nematic liquid crystal MDA-06-177 (Merck, $\Delta n = 0.143$, $T_{NI} = 100^\circ C$) was filled at room temperature, and annealed at $120^\circ C$ for 5 min. The reflective substrate consisted of either an Al mirror (Edmund

Optics), or a 256x256 pixel Si backplane (24 μm pixel width/height, Boulder Nonlinear Systems). In all cases, excellent quality gratings were formed with low scattering (< 1%).

4. Results

We will first consider results from LCPGs formed on Al mirrors, wherein we expect our best results since the reflective substrate is uniform (i.e. no topography or structure to influence the hologram formation or degrade diffractive behavior). Several definitions will be helpful as we characterize the inherent properties of LCPGs: (i) *grating efficiency* $\eta_m = I_m / (\dots + I_{-1} + I_0 + I_1 + \dots)$, is a normalized term that describes the inherent diffraction behavior of the LCPG layer alone, and is directly comparable to Eq. (1); (ii) total first-order *reflectance* $R = (I_{-1} + I_1) / I_{\text{IN}}$ is a true (un-normalized) measure including all substrate, interface, and grating effects; and (iii) full-on-full-off *contrast ratio*, defined as $I_{\text{ON}} / I_{\text{OFF}}$. In each of these, I_m is the measured intensity of the m^{th} reflected diffraction order, I_{IN} is the incident intensity, and $I_{\text{ON/OFF}}$ is the maximum/minimum total first-order incident intensity. Electro-optic measurements on mirror-substrates involved a 4 kHz square wave (with zero DC bias), while those for the microdisplay employed a 120 Hz sub-frame (field) rate.

4.1 Reflective LCPGs On Mirrors

The voltage response of a reflective LCPG ($\Lambda=2.5\mu\text{m}$, $d=1.4\mu\text{m}$) formed on an Al mirror is shown in Fig. 2a. The grating efficiency and reflectance (of the first-orders) was measured with a HeNe laser (633 nm) and with unpolarized LEDs (collimated for this measurement to about $\pm 4^\circ$). We observe that the LCPG diffracted the laser with $\Sigma\eta_{\pm 1}=94\%$, appreciably near the 100% theoretical value. Perhaps more prominently, the red LED produced a high peak efficiency $\Sigma\eta_{\pm 1}=85\%$ and reflectance $R=75\%$ at 2.4V (with slightly lower values for green and blue LEDs). These losses are predominantly due to air-glass interface and electrode-absorption losses. Crucially, this reflectance is significantly higher than any reflective LC microdisplay (e.g. VAN-mode) that employs polarizers. As expected, the applied voltage reduced the diffraction.

The dynamic response was also measured, where a sub-ns total switching times are typical [4], clearly enabling field-sequential-color operation. Fig. 2b shows the rise and fall times (10%-90% transitions) of the LCPG switching from 0V to the indicated applied voltage. While the overall speed (< 800 μs) of this nematic LC configuration is comparably fast, the general trend is similar to other LC modes: rise-time is strongly dependent on voltage, while fall-time is roughly constant.

As can be deduced from Fig 2a, the dark state results from a high voltage (i.e. a drive-to-black configuration), and is crucially dependent on the interaction between the applied voltage and the surface anchoring strength. The contrast measured on two of our best samples ($\Lambda=4.0\mu\text{m}$, $d=1.6\mu\text{m}$, MLC-12100-000) is shown in Fig. 2c, along with the typical range values. We observed that for at least some of our samples, contrasts approaching 1000:1 are possible at modest operating voltages of ~ 22 V. Note that we are currently focusing our materials optimization effort on higher contrast at lower voltages with small grating periods ($\leq 2.5\mu\text{m}$).

4.2 Reflective LCPG Microdisplay

The voltage response of a reflective LCPG ($\Lambda=2.6\mu\text{m}$, $d=1.4\mu\text{m}$) formed on a 256x256 pixel Si backplane is shown in Fig. 3. The grating efficiency behavior is substantially similar to Fig. 2 (<80%), with maxima that are only slightly lower, implying that a

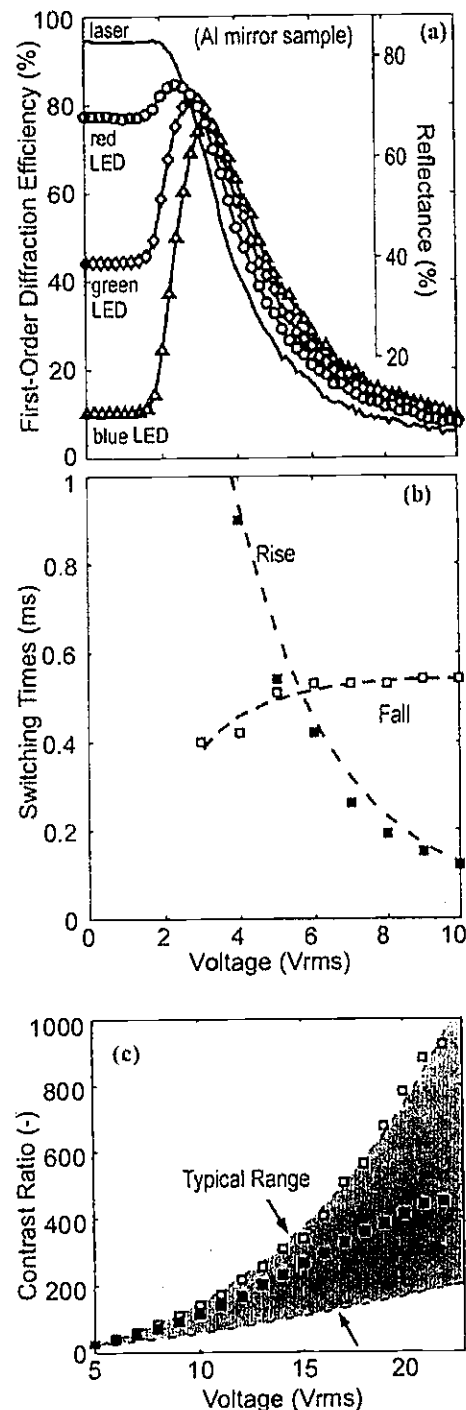


Figure 2 – Electro-optic behavior of Reflective LCPGs formed on Al mirrors: Voltage response (a) of grating efficiency and reflectance (inset); (b) Sub-ns switching times; and (c) Contrast ratio of the first-order diffraction of a HeNe laser (633 nm). (For parts (a) & (b), $\Lambda = 2.5 \mu\text{m}$ and $d = 1.4 \mu\text{m}$, and in part (c), $\Lambda = 4.0 \mu\text{m}$ and $d = 1.6 \mu\text{m}$)

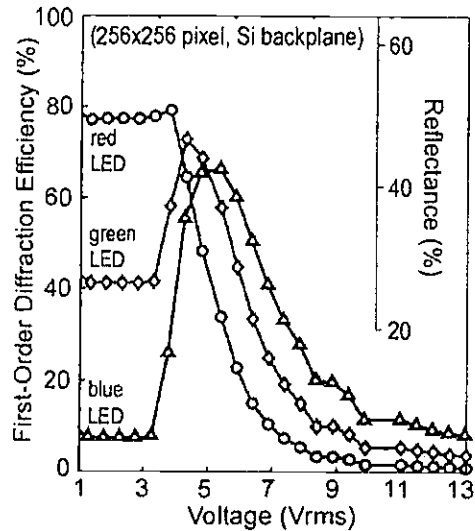


Figure 3 – Electro-optic behavior of LCPG microdisplay (256x256): Voltage response of the efficiency and reflectance. ($\Lambda = 2.6 \mu\text{m}$ and $d = 1.4 \mu\text{m}$)

good quality grating was also created on the pixelated backplane. We note, however, that the peak reflectance in this case overall is lower (~50%), which we attribute to several effects: a lower overall reflectance of the pixel mirror, the loss associated with the pixel fill-factor, and any diffractive coupling between the pixel-array and the LCPG itself. While we do not fully understand this currently, we continue to investigate this. It is important to note that the switching times are essentially identical to Fig. 2b.

4.3 Prototype Projector

Since the LCPG microdisplay reflects the zero- and first-order with $\sim 14^\circ$ separation, we can implement a polarizer-free projector (Fig. 1c and Table 1) as a proof-of-principle. We employ (Fig. 4a) an LED light source ($\sim 90 \text{ lm}$ at $\sim 8.3 \text{ W}$, Goldeneye Inc.) with simple optics and use field-sequential-color. Note the extreme simplicity of the optical 'guts' of the projector, with only a few lenses and a fold-mirror (serving also as the aperture stop). An actual image is also shown in Fig. 4b. This admittedly sub-optimal projector platform nevertheless supports video (120 Hz field-rate), presents good color saturation (by eye), sends $\sim 15 \text{ lm}$ to the screen, manifests 50:1 contrast for the red LED (within the 13V capability), and has an overall efficacy of $\sim 1.8 \text{ lm/W}$. It is clear that most of the losses and the poor contrast are due to unsuitable lens choices and alignment, and we actively continue to improve on this toward a goal of $> 8 \text{ lm/W}$ and much higher contrast.

5. Conclusion

We have developed a polarization-independent, diffractive, LC microdisplay on a reflective silicon backplane, and implemented a prototype projection system with an LED light source using field-sequential-color. The approach combines the low cost of a single LCuS panel and the high efficiency of DLPTM, and the technology enables ultra-portable, low-power, compact projection displays. While several competing "Pocket Projector" approaches are emerging, our microdisplay technology represents a dramatic potential advantage with respect to cost, simplicity, and power savings. Furthermore, because the technology is scalable in resolution, front-projectors are also an attractive application.

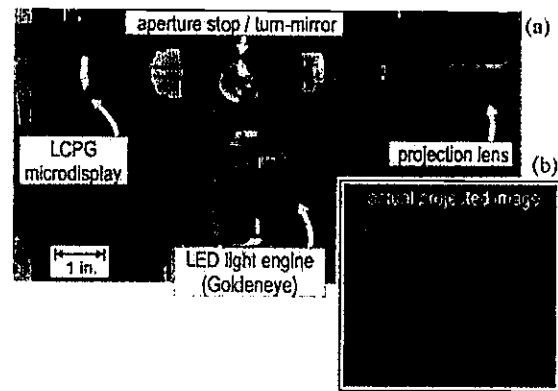


Figure 4 – Polarizer-free projector prototype based on LCPGs: (a) Photo of the simple projector system, with three lenses, a fold-mirror, LEDs, and projection lens; and (b) A projected image (from "Ice Age 2" movie, 20th Century Fox).

6. Acknowledgements

The authors gratefully acknowledge the support of the National Science Foundation (ECCS-0621906) and the Kenan Institute for Engineering, Technology, and Science. We also thank Boulder Nonlinear Systems Inc. and Goldeneye Inc. for deep technical support in integrating LCPG technology with the LCuS backplane and for providing the light-recycling LED source, respectively.

6. References

- [1] M. J. Escuti, W. M. James, *SID Symp. Digest*, vol. 37, pp. 1443-1446 (2006).
- [2] W. M. James, B. L. Conover, M. J. Escuti, *SID Symp. Digest*, vol. 37, pp. 1015-1018 (2006).
- [3] R. Komanduri et al., *J. Soc. Inf. Displ.*, vol. 15, pp. 589-594 (2007).
- [4] R. Komanduri, M. J. Escuti, *Phys. Rev. E*, vol. 76, pp. 021701 (2007).
- [5] D.-K. Yang, *J. Soc. Inf. Displ.*, vol. 16, pp. 117-124 (2008).
- [6] J. Chen et al., *Appl. Phys. Lett.*, vol. 67, pp. 2588-2590 (1995).
- [7] C. M. Titus, P. J. Bos, *Appl. Phys. Lett.*, vol. 71, pp. 2239-2241 (1997).
- [8] M. Honma, T. Nuse, *Appl. Opt.*, vol. 43, pp. 5193-5197 (2004).
- [9] J. Eakin et al., *Appl. Phys. Lett.*, vol. 85, pp. 1671-1673 (2004).
- [10] H. Sarkissian et al., *Opt. Lett.*, vol. 31, pp. 2248-2250 (2006).
- [11] L. Nikolova, T. Todorov, *Optica Acta*, vol. 31, pp. 579-588 (1984).
- [12] P. Yeh, C. Gu, *Optics of Liquid Crystal Displays* (John Wiley & Sons, Inc., New York, 1999).
- [13] M. Schadt, H. Seiberle, A. Schuster, *Nature*, vol. 381, pp. 212-215 (1996).